Characterization of a 0.35-Micron-Based Analog MPPT IC at Various Process Corners

Lean Karlo Tolentino[1], Febus Reidj Cruz[2,3], Wen-Yaw Chung[3]
[1]*Electronics Engineering Department, College of Engineering, Technological University of the Philippines, Manila, Philippines*
[2]*Mapua Institute of Technology, School of Electrical, Electronics, and Computer Engineering, Manila, Philippines*
[3]*Department of Electronic Engineering, Chung Yuan Christian University, Chungli City, Taiwan R.O.C.*
leankarlo_tolentino@tup.edu.ph

***Abstract*—An analogue maximum power point tracking (MPPT) controller integrated circuit (IC) based on ripple correlation control was modified for low voltage applications in this study to harvest the maximum power from the photovoltaic array or solar panel under partial shading and changes in temperature. The IC was implemented in TSMC 0.35um 2P4M 5V mixed-signal CMOS technology. It was simulated at various process corners namely: typical-typical (TT); slow-slow (SS); fast-fast (FF); slow-fast (SF); and fast-slow (FS). The simulation results showed that at a 400 W/m^2 solar irradiance and 25 degrees Celsius temperature, the tracking efficiencies are 99.18%, 98.55%, 98.89%, 98.96%, and 98.90% at different process corners, TT, FF, FS, SF, and SS, respectively.**

***Index Terms*—MPPT; Process Corners; Solar Panel; Tracking Efficiency.**

I. INTRODUCTION

Maximum power point tracking (MPPT) is a method used to harvest power from photovoltaic cells (PV) matching them with the load or battery so that maximum power is guaranteed [1]. It is best used at varying solar irradiance or partial shading (during rainy and cloudy conditions) and cell temperature (during hot and cold weather).

MPPT controller circuits which are implemented using analogue circuits are low in cost and small in size than implemented using digital circuits [2]. As an analog only implementation, the ripple correlation control algorithm [3]-[12] (RCC) is chosen for the MPPT controller because it uses the principle of the product (analog multiplier circuit implementation) of the derivative (differentiator circuit) of the sensed PV power and the derivative of the sensed PV voltage with respect to time. It uses comparator circuits to convert the output from the differentiator circuits to two voltage levels which may represent logic 1 (increasing power or current) and logic 0 (decreasing). The outputs from the comparators are processed by an XNOR gate which determines if the voltage of the PV cell must be increased or decreased by letting the switch (Power MOSFET) of the dc-dc converter to be opened until the sensed power from the PV cell decreases. Then, the switch will close which in turn decreases the sensed voltage until an estimated tracked maximum power point is located making the switch opens and closes rapidly (varying the duty cycle of the dc-dc converter at regular intervals of time. The flowchart in Figure 1 represents the RCC principle.

The general objective of this paper is to design a maximum power point tracking controller IC. Specifically, it aims to design an equivalent integrated circuit of the MPPT controller using TSMC 0.35 um 2P4M 3.3/5V mixed-signal CMOS technology.

This study was limited to the development of a 5V MPPT controller IC that can track maximum power at irradiance levels 400, 600, 800, and 1000 W/m^2. It also applied at different temperature levels 20, 25, and 30 degrees Celsius, and at different process corners typical-typical (TT), slow-slow (SS), fast-fast (FF), slow-fast (SF), and fast-slow (FS).

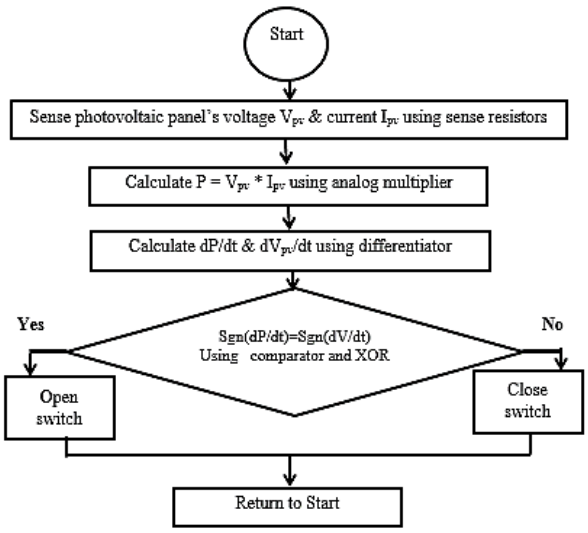

Figure 1: RCC MPPT algorithm flowchart

II. PHOTOVOLTAIC ARRAY

Photovoltaic cells consist of a p-n junction which, when sensitive to light, releases electrons. From this principle, the photovoltaic cell can be modelled similarly to the equivalent circuit shown in Figure 2. The current source I_{ph} represents the light generated from the photovoltaic cell. The diode represents the intrinsic p-n junction characteristic. The shunt resistance R_{sh} represents the leakage current in the cell while series resistance R_s represents the intrinsic resistance the electrons face before reaching the cell's electrical contacts. The value of R_{sh} is very large while R_s is very small. Usually, a solar panel consists of n_s number of well-matched PV cells in series and n_p number of cells in parallel. The total shunt resistance and the total series resistance of the solar panel are equal to the product of n_s and R_{sh} and the product of n_s and R_s. The IV characteristic of a single photovoltaic cell, which is the relationship between photovoltaic voltage V_{cell} and

photovoltaic cell current I_{cell} is defined by:

$$I_{cell} = I_{ph} - I_s[\exp(\alpha(V_{cell} + I_{cell}R_s))-1] - \frac{V_{cell} + I_{cell}R_s}{R_{sh}} \quad (1)$$

where $\alpha = 1/(n\ V_T) = 1/uvet$ where n is the ideality diode constant, $V_T = q/(k*T)$, k is the Boltzmann's constant, T is absolute temperature, q is the electron charge and I_s is diode's saturation current [13].

It is assumed that shunt resistance R_{sh} is very large and its effects can be ignored and $I_{sc} = I_{ph}$, equation 1 becomes:

$$I_{cell} = I_{sc} - I_s[e^{\left(\frac{(V_{cell} + I_{cell}R_s)}{nV_T}\right)}-1] \quad (2)$$

From Castañer and Silvestre's equations [13], the scaling rules of voltages, currents, and resistances when a matrix of n_s by n_p solar cells is considered are the following:

$$I_M = N_p I_{cell} \quad (3)$$

$$I_{scM} = N_p I_{sc} \quad (4)$$

$$V_M = N_s V_{cell} \quad (5)$$

$$V_M = N_s V_{cell} \quad (6)$$

where "M stands for 'Module' and subscript cell stand for a single solar cell. The scaling rule of the series resistance R_s is the same as that of an N_s by N_p association of resistors:"

$$R_{sM} = \frac{N_s}{N_p} R_s \quad (7)$$

Substituting in Equation (1),

$$\frac{I_M}{N_p} = \frac{I_{scM}}{N_p} - I_s[e^{\left(\frac{\frac{V_M}{N_s} + \frac{I_M N_p}{N_p N_s} R_{sM}}{nV_T}\right)}-1] \quad (8)$$

$$I_M = I_{scM} - N_p I_s[e^{\left(\frac{V_M + I_M R_{sM}}{nN_s V_T}\right)}-1] \quad (9)$$

From Equation (2) in an open circuit, I_s is:

$$I_s = \frac{I_{sc}}{e^{\left(\frac{V_{oc}}{nV_T}\right)}-1} \quad (10)$$

$$I_s = \frac{I_{scM}}{N_p\left[e^{\left(\frac{V_{ocM}}{nN_s V_T}\right)}-1\right]} \quad (11)$$

They [13] added that the fill factor FF of the solar panel is:

$$FF_{0M} = \frac{v_{oc} - \ln(v_{oc} + 0.72)}{1 + v_{oc}} \quad (12)$$

where normalised value v_{oc} is:

$$v_{oc} = \frac{V_{oc}}{nV_T} = \frac{V_{ocM}}{nN_s V_T} \quad (13)$$

The series resistance is calculated from the value of the power density per unit area at the maximum power point.

$$P_{maxM} = FF_M\ V_{ocM}\ J_{scM} = FF_{0M}\ (1-R_{sM})\ V_{ocM}\ J_{scM} \quad (14)$$

and

$$R_{sM} = \frac{V_{ocM}}{I_{scM}} - \frac{P_{maxM}}{FF_{0M} I^2_{scM}} \quad (15)$$

The equations are converted into HSPICE netlist corresponding to schematics as shown below.

HSPICE netlist for the photovoltaic array model

```
1   *solar panel subcircuit
2   .subckt PV 400 403 402 ta=1
3   +tr='TEMPERATURE' iscmr=2.04
4   +pmaxmr=32 vocmr=21.72 ns=36 np=1
5   + nd=1
6   girradm 400 401
7   + value='(iscmr/1000*v(402))'
8   d1 401 400 diode
9   .model diode d(is='iscmr/(np*exp
10  +(vocmr/(nd*ns*(8.66e-5*(tr+273)))))'
11  +, n='nd*ns')
12  .param uvet='8.66e-5*(tr+273)'
13  .param vocnorm='vocmr/(nd*ns*uvet)'
14  .param rsm='vocmr/(iscmr)-pmaxmr*
15  +*(1+vocnorm)/((iscmr^2)*(vocnorm-
16  + log((vocnorm)+0.72)))'
17  rs 401 403 'rsm'
18  .ends
```

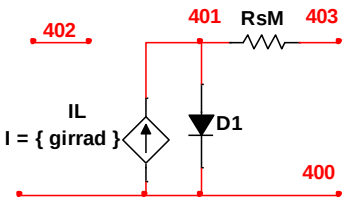

Figure 2: Equivalent circuit for the PV module subcircuit [13].

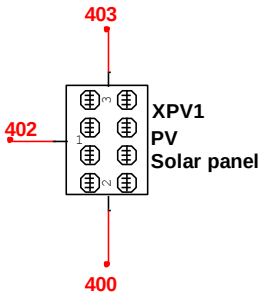

Figure 3: SPICE model for the PV module subcircuit [13].

From the HSPICE netlist of the photovoltaic array model as shown in Figure 3, parameters or characteristics of the

solar panel which are typically found in specification sheets can be inputted directly. Those parameters are:

- The ambient temperature (ta at 25 ^{0}C)
- the operating temperature of the cells (tr which is variable)
- the photovoltaic module's short-circuit current I_{sc} (iscmr)
- the photovoltaic maximum power rating Pmax at standard temperature (normally at 25^{0}C (pmaxmr))
- the photovoltaic module's open-circuit voltage V_{oc} (vocmr)
- the number of cells in series n_s e.g. for a 12V solar panel, it usually has 36 cells, the number of cells in parallel n_p, and
- the ideality constant of the diode n_d. Nodes 403 and 400 are the positive and negative nodes of the voltage supply of the solar panel.

Meanwhile, node 402 is a testing node which is connected to a virtual dc voltage source which represents the solar irradiance or irradiance measured in watts per square meter.

III. Characterization of the Photovoltaic Array Model

The HSPICE model of the photovoltaic array can be characterised and simulated to plot the power-voltage characteristic and the current-voltage characteristic of the array at different temperatures and solar irradiances. It is also used for the testing of the MPPT controller.

Figure 4 shows the setup for the characterisation of the power-voltage characteristic and the current-voltage characteristic of the solar panel. A dc sweep analysis is done at voltage source Vbias starting at 0V to a value close to the open-circuit voltage (22V). The inverse of the power at Vbias (-P(VBIAS)) and the current at Vbias (I(VBIAS)) are plotted to generate the characteristic curves and determine the maximum power at different temperatures and solar irradiances.

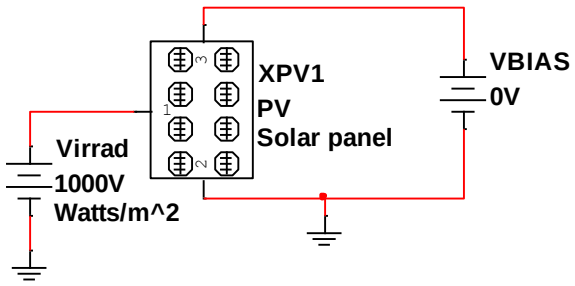

Figure 4: Setup for the characterisation of the power-voltage characteristic and the current-voltage characteristic of the solar panel

IV. Simulation Results Of The Photovoltaic Model Characterization

Figure 5 shows the power-voltage P-V characteristic curve of the photovoltaic panel model under varying irradiances (400, 600, 800, and 1000 W/m^2) at 25 degrees Celsius, respectively using HSPICE Avanwaves. Meanwhile, Figure 6 shows the current-voltage I-V characteristic curve of the photovoltaic panel model under varying irradiances (400, 600, 800, and 1000 W/m^2) at 25 degrees Celsius, respectively. From these figures, the red, yellow, green, and blue curves represent P-V or I-V curves at 400, 600, 800, and 1000 W/m^2, respectively.

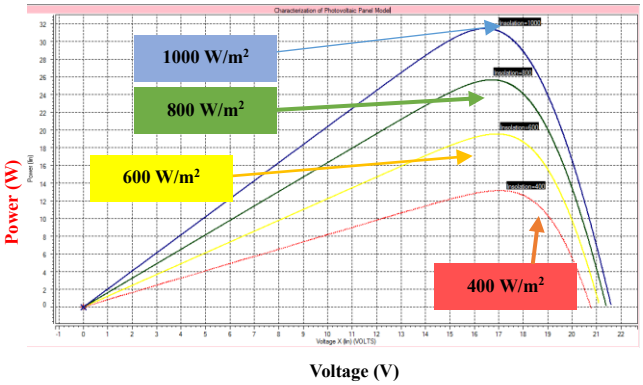

Figure 5: Power-voltage P-V characteristic curve of the photovoltaic panel model under varying irradiances (400, 600, 800, and 1000 W/m^2) at 25 degrees Celsius.

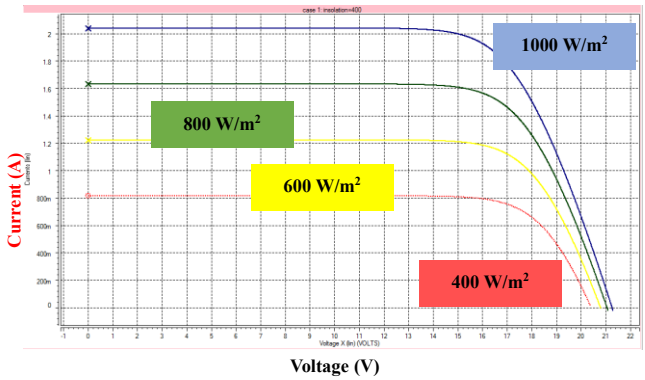

Figure 6: Current-voltage I-V characteristic curve of the photovoltaic panel model under varying irradiances (400, 600, 800, and 1000 W/m^2) at 25 degrees Celsius.

Meanwhile, Tables 1, 2, and 3 summarise the values of the ideal maximum power (P_{max}), the voltage (V_{mp}), and the current (I_{mp}) at maximum power. The data are based on the power-voltage P-V characteristic curve of the photovoltaic panel model of Figures at solar cell temperatures, 20, 25, and 30 degrees Celsius, respectively.

Table 1
Voltages (V_{mp}) and Currents (I_{mp}) at Maximum Power and the Ideal Maximum Power (P_{max}) Extracted from the Power-Voltage P-V and Current-Voltage I-V Characteristic Curves for Different Solar Irradiances/Irradiances at 20^{0}C Solar Cell Temperature.

Irradiance (W/m^2)	Voltage At Maximum Power V_{mp} (V)	Current At Maximum Power I_{mp} (A)	Ideal Maximum Power P_{max} (W)
400	17.37	0.772	13.411
600	17.25	1.155	19.93
800	17.03	1.536	26.161
1000	16.76	1.914	32.076

Table2
Voltages (V_{mp}) and Currents (I_{mp}) at Maximum Power and the Ideal Maximum Power (P_{max}) Extracted from the Power-Voltage P-V and Current-Voltage I-V Characteristic Curves for Different Solar Irradiances/Irradiances at 25^0 C Solar Cell Temperature.

Irradiance (W/m^2)	Voltage At Maximum Power V_{mp} (V)	Current At Maximum Power I_{mp} (A)	Ideal Maximum Power P_{max} (W)
400	17.03	0.771	13.14
600	16.92	1.154	19.536
800	16.71	1.535	25.65
1000	16.45	1.912	31.456

Table 3
Voltages (V_{mp}) and Currents (I_{mp}) at Maximum Power and the Ideal Maximum Power (P_{max}) Extracted from the Power-Voltage P-V and Current-Voltage I-V Characteristic Curves for Different Solar Irradiances/Irradiances at 30^0 C Solar Cell Temperature.

Irradiance (W/m^2)	Voltage At Maximum Power V_{mp} (V)	Current At Maximum Power I_{mp} (A)	Ideal Maximum Power P_{max} (W)
400	16.71	0.770	12.879
600	16.61	1.153	19.155
800	16.41	1.533	25.158
1000	16.16	1.910	30.859

V. THE MPPT CONTROLLER IC

Figures 7, 8, and 9 show the setup for the MPPT controller IC. As shown in Figure 7, the IPV pin (input of inverting amplifier CURSEN AMP as shown in Figure 10) through the 0.7-ohm current sense resistor converts the current from the PV cell/panel to a voltage value. Meanwhile, the VPV pin (input of voltage follower VOLSEN AMP as shown in Figure 10) through the resistor network of voltage dividers senses the photovoltaic voltage parameter V_{pv}. The product of sensed voltage and current values from the CURSEN and VOLSEN amp to have a power parameter value are done by the MULT block (analogue multiplier as shown in Figures 10 and 13). The output of the MULT block is then fed to the instrumentation amplifier INAMP to amplify the differential signal from the MULT block. The derivatives of the sensed voltage from VOLSEN AMP and the output from the INAMP are processed by the differentiator circuits DIFFAMP 1 and DIFFAMP 2. Their outputs are then connected to the comparators COMP A and COMP B so that the XNOR to have inputs of logic 0 or 1 instead of +V/-V from the DIFFAMP blocks. The output of the XOR commands the D flip-flop DFF block to trigger the switch (Power MOSFET) using GATE pin to open or close. The DFF block is clocked by the OSC block (three-gate oscillator) at 10 KHz. VDD (+2.5V), VSS (-2.5V), and V5 (+5V) pins are pins of the supplies of the MPPT controller IC.

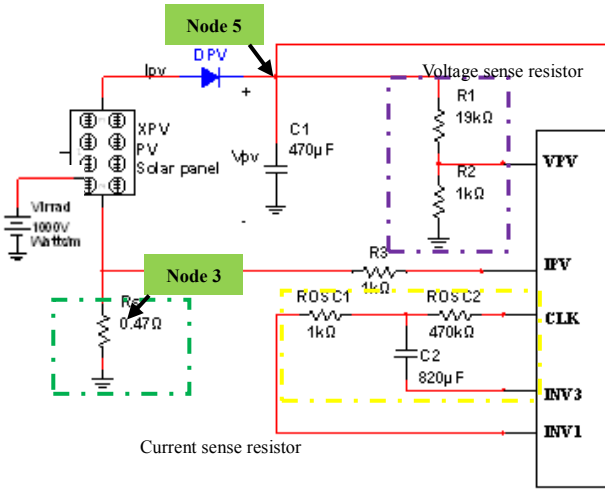

Figure 7: Inputs to the MPPT controller IC

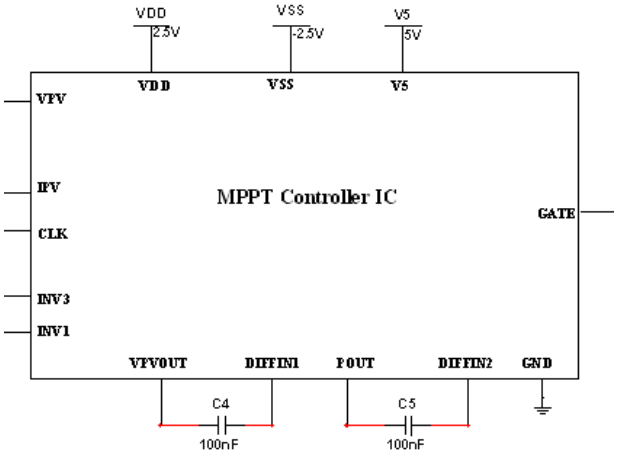

Figure 8: MPPT controller IC

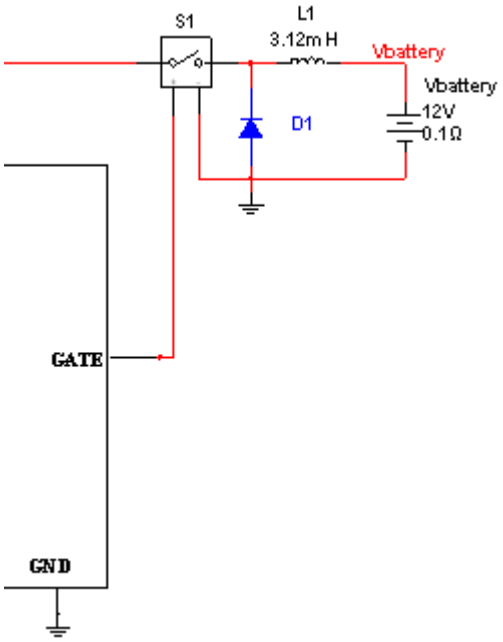

Figure 9: Output to the MPPT controller IC

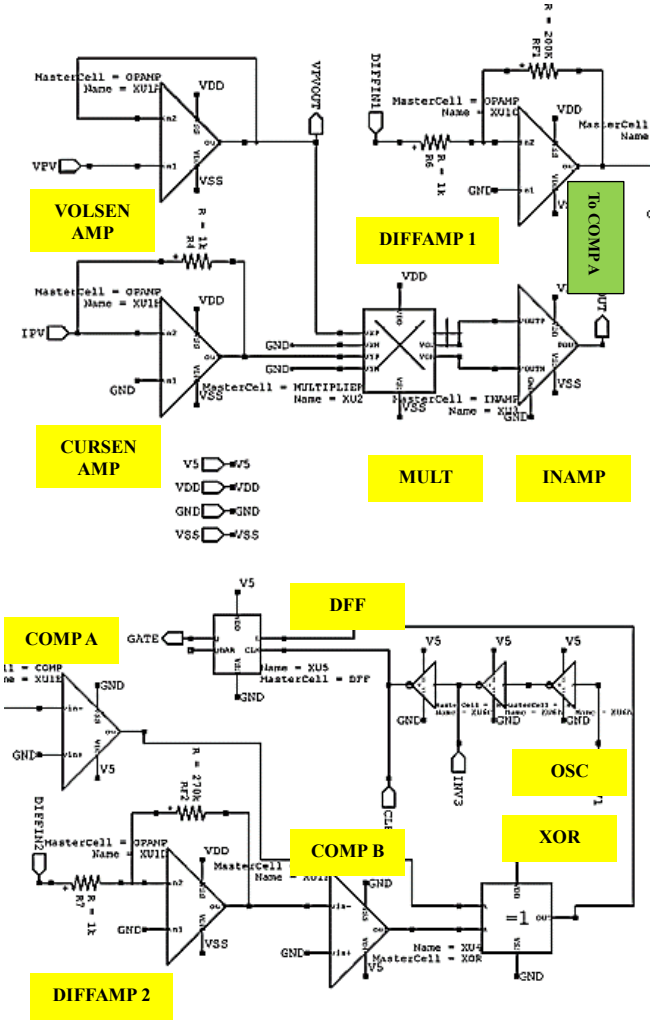

Figure 10: MPPT controller schematic diagram

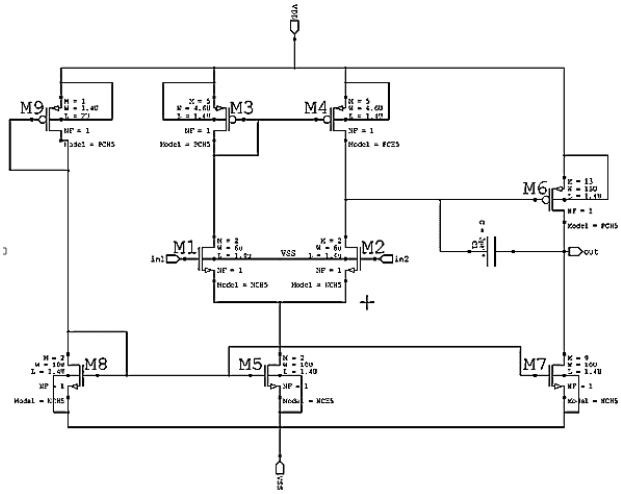

Figure 11: Two-stage operational amplifier circuit (VOLSEN AMP and CURSEN AMP) for the voltage/current sensors and instrumentation amplifier block (INAMP)

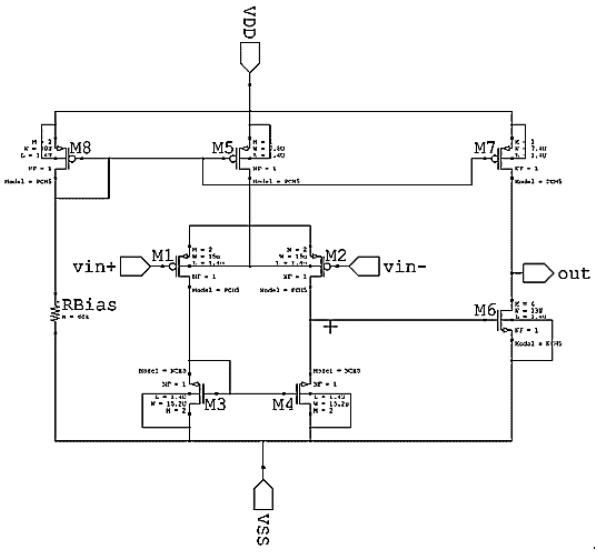

Figure 12: PMOS input-driven two-stage comparator circuit (COMP A and COMP B)

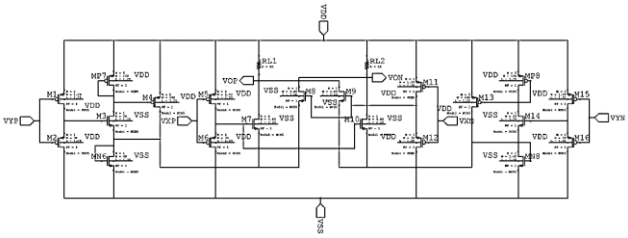

Figure 13: Analogue multiplier circuit (MULT)

The values of off-chip resistances ROSC1 and ROSC2 and capacitances C2 which are connected to the OSC block to generate 10 kHz frequency is computed using the formula:

$$f = \frac{1}{2C\,(0.693R_1 + 0.405R_{eq})} \tag{16}$$

where R_{eq} equals:

$$R_{eq} = \frac{R_1 R_2}{R_1 + R_2} \tag{17}$$

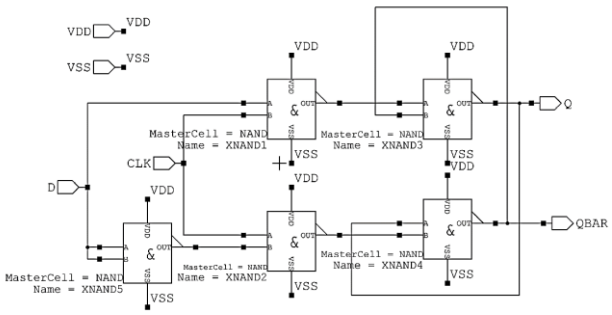

Figure 14: D flip-flop (DFF) using NAND CMOS gates

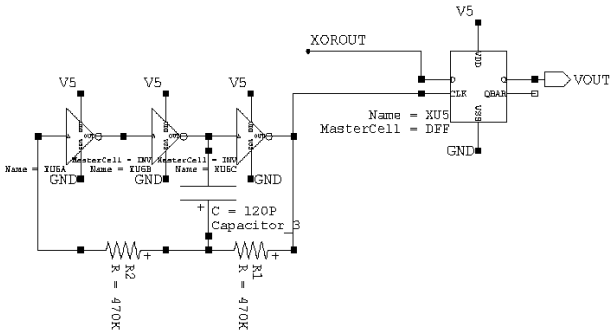

Figure 15: Three-gate oscillator (OSC) connected to DFF

VI. Process Corner Simulations

Corners describe changes due to process inaccuracies, e.g. doping variations, temperature and other parameter variations. Simulations that yield these variances into consideration vary. Process corners are supplied with the process design kit (PDK), e.g. TSMC 0.35um 2P4M and are within models library. For example, the PDK includes corners for Fast NMOS-Fast PMOS (FF), Slow NMOS-Slow PMOS (SS), Fast NMOS-Slow PMOS (FS), Slow NMOS-Fast PMOS (SF), and Typical NMOS-Typical PMOS (TT). During corner simulation, all available corners were simulated using HSPICE and effect of parameter/process variations on IC can be determined.

With temperature fixed at 20^0C and solar irradiance (represented as a voltage source Virrad) at 400W/m^2, the test setup as shown in Figure 7 was simulated using transient analysis in HSPICE while the process corners (TT, FF, FS, SS, and SF) are considered. The waveform of the duty cycle at pin GATE was observed. The photovoltaic voltage and power at node (5,3) were measured by taking their average values when the time is from 18ms to 22ms, and their waveforms were recorded. The simulation and procedure were repeated, but the irradiance is changed from 400W/m^2 to 600W/m^2, 800W/m^2, and 1000 W/m^2.

The temperature was modified to 25^0C and 30^0C while repeating the procedure in the paragraph above to observe the behaviour of the waveforms when the temperature was changed.

The measured values of the tracked photovoltaic power from procedures of the last two paragraphs were compared from the theoretical maximum power values of the photovoltaic SPICE model. Then, the tracking efficiency of the MPPT controller at different conditions was computed using the formula:

$$\eta_{track} = \frac{P_{out}}{P_{max}} \times 100\% \qquad (18)$$

where P_{out} is the output power tracked or produced by the photovoltaic panel under the control of the MPPT. P_{max} is the theoretical maximum power of the photovoltaic panel.

A summary of waveforms of the tracked power from the photovoltaic panel for different irradiances of 400 (green), 600 (blue), 800 (violet), and 1000 (red) W/m^2 at temperatures of 25 degrees Celsius and different process corners were illustrated using HSPICE Avanwaves in Figures 16 to 20. The values of the tracked power at 20, 25, and 30 degrees Celsius were recorded and compared with the values of the ideal maximum power in Tables 4 to 19. The tracking efficiencies were calculated, and their values are above 90%. It can be observed that the system is tracking the maximum power point precisely as the tracking efficiency is nearing 100%.

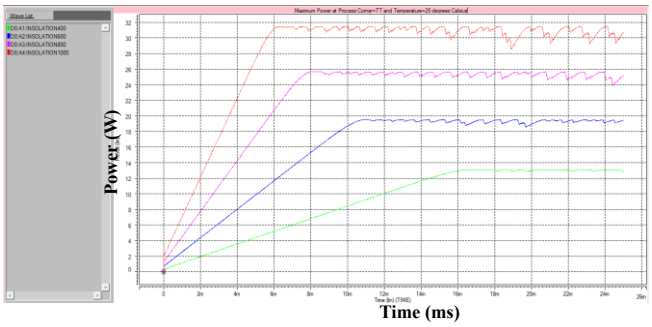

Figure 16: Photovoltaic array power of the MPPT Controller IC at node V(5,3) for different solar irradiances at 25^0 C solar cell temperature. Corner Case: Typical-Typical (TT)

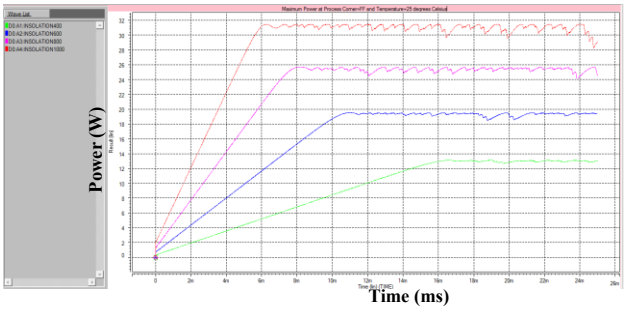

Figure 17: Photovoltaic array power of the MPPT Controller IC at node V(5,3) for different solar irradiances at 25^0 C solar cell temperature. Corner Case: Fast-Fast (FF)

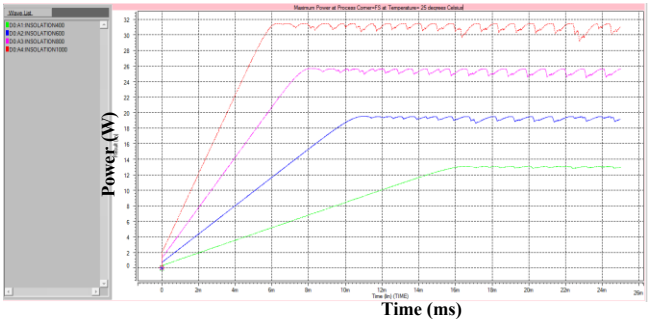

Figure 18: Photovoltaic array power of the MPPT Controller IC at node V(5,3) for different solar irradiances at 25^0 C solar cell temperature. Corner Case: Fast-Slow (FS)

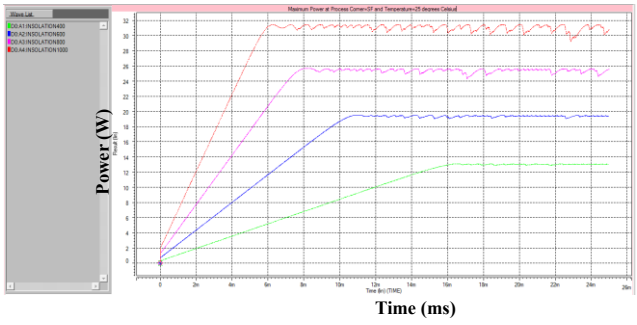

Figure 19: Photovoltaic array power of the MPPT Controller IC at node V(5,3) for different solar irradiances at 25^0 C solar cell temperature. Corner Case: Slow-Fast (SF)

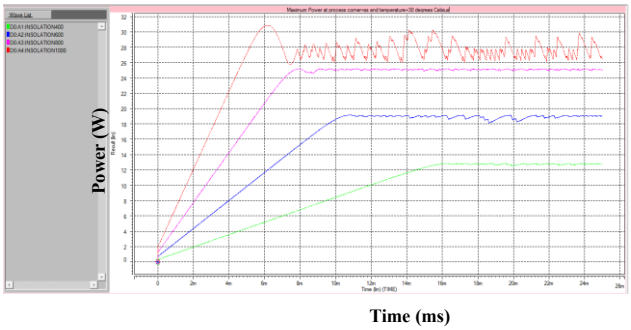

Figure 20: Photovoltaic array power of the MPPT Controller IC at node V(5,3) for different solar irradiances at 25^0 C solar cell temperature. Corner Case: Slow-Slow (SS)

Table 4
Photovoltaic Array Power of the MPPT Controller IC at Node V(5,3) for Different Solar Irradiances at 20^0 C Solar Cell Temperature. Corner Case: Typical-Typical (TT)

Irradiance (W/m^2)	Ideal Maximum Power (W)	Measured Actual Power (W)	Tracking Efficiency (%)
400	13.411	13.2880	99.08%
600	19.93	19.7094	98.89%
800	26.161	25.5616	97.71%
1000	32.076	31.4098	97.92%

Table 5
Photovoltaic Array Power of the MPPT Controller IC at node V(5,3) for Different Solar Irradiances at 25^0 C Solar Cell Temperature. Corner Case: Typical-Typical (TT)

Irradiance (W/m^2)	Ideal Maximum Power (W)	Measured Actual Power (W)	Tracking Efficiency (%)
400	13.14	13.0325	99.18%
600	19.536	19.2598	98.59%
800	25.65	25.3317	98.76%
1000	31.456	30.6452	97.42%

Table 6
Photovoltaic Array Power of the MPPT Controller IC at node V(5,3) for Different Solar Irradiances at 30^0 C Solar Cell Temperature. Corner Case: Typical-Typical (TT)

Irradiance (W/m^2)	Ideal Maximum Power (W)	Measured Actual Power (W)	Tracking Efficiency (%)
400	12.879	12.7771	99.21%
600	19.155	18.8907	98.62%
800	25.158	24.7861	98.52%
1000	30.859	30.2815	98.13%

Table 7
Photovoltaic Array Power of the MPPT Controller IC at node V(5,3) for Different Solar Irradiances at 20^0 C Solar Cell Temperature. Corner Case: Fast-Fast (FF)

Irradiance (W/m^2)	Ideal Maximum Power (W)	Measured Actual Power (W)	Tracking Efficiency (%)
400	13.411	13.2798	99.02%
600	19.93	19.6011	98.35%
800	26.161	25.6807	98.16%
1000	32.076	31.1781	97.20%

Table 8
Photovoltaic Array Power of the MPPT Controller IC at node V(5,3) for Different Solar Irradiances at 25^0 C Solar Cell Temperature. Corner Case: Fast-Fast (FF)

Irradiance (W/m^2)	Ideal Maximum Power (W)	Measured Actual Power (W)	Tracking Efficiency (%)
400	13.14	12.9491	98.55%
600	19.536	19.1614	98.08%
800	25.65	25.4477	99.21%
1000	31.456	30.9711	98.46%

Table 9
Photovoltaic Array Power of the MPPT Controller IC at node V(5,3) for Different Solar Irradiances at 30^0 C Solar Cell Temperature. Corner Case: Fast-Fast (FF)

Irradiance (W/m^2)	Ideal Maximum Power (W)	Measured Actual Power (W)	Tracking Efficiency (%)
400	12.879	12.7599	99.08%
600	19.155	18.7285	97.78%
800	25.158	24.8698	98.85%
1000	30.859	30.6546	99.34%

Table 10
Photovoltaic Array Power of the MPPT Controller IC at node V(5,3) for Different Solar Irradiances at 20^0 C Solar Cell Temperature. Corner Case: Fast-Slow (FS)

Irradiance (W/m^2)	Ideal Maximum Power (W)	Measured Actual Power (W)	Tracking Efficiency (%)
400	13.411	13.2171	98.55%
600	19.93	19.5436	98.06%
800	26.161	25.7361	98.38%
1000	32.076	31.6084	98.54%

Table 11
Photovoltaic Array Power of the MPPT Controller IC at node V(5,3) for Different Solar Irradiances at 25^0 C Solar Cell Temperature. Corner Case: Fast-Slow (FS)

Irradiance (W/m^2)	Ideal Maximum Power (W)	Measured Actual Power (W)	Tracking Efficiency (%)
400	13.14	12.9948	98.89%
600	19.536	19.2143	98.35%
800	25.65	25.2508	98.44%
1000	31.456	31.0085	98.58%

Table 12
Photovoltaic Array Power of the MPPT Controller IC at node V(5,3) for Different Solar Irradiances at 30^0 C Solar Cell Temperature. Corner Case: Fast-Slow (FS)

Irradiance (W/m^2)	Ideal Maximum Power (W)	Measured Actual Power (W)	Tracking Efficiency (%)
400	12.879	12.7341	98.87%
600	19.155	18.8277	98.29%
800	25.158	24.7860	98.52%
1000	30.859	30.4635	98.72%

Table 13
Photovoltaic Array Power of the MPPT Controller IC at node V(5,3) for Different Solar Irradiances at 20^0 C Solar Cell Temperature. Corner Case: Slow-Fast (SF)

Irradiance (W/m^2)	Ideal Maximum Power (W)	Measured Actual Power (W)	Tracking Efficiency (%)
400	13.411	13.2754	98.99%
600	19.93	19.7299	99.00%
800	26.161	25.6952	98.45%
1000	32.076	31.5062	98.22%

Table 14
Photovoltaic Array Power of the MPPT Controller IC at node V(5,3) for Different Solar Irradiances at 25^0 C Solar Cell Temperature.
Corner Case: Slow-Fast (SF)

Irradiance (W/m^2)	Ideal Maximum Power (W)	Measured Actual Power (W)	Tracking Efficiency (%)
400	13.14	13.0038	98.96%
600	19.536	19.3829	99.21%
800	25.65	25.4005	99.02%
1000	31.456	30.9910	98.52%

Table 15
Photovoltaic Array Power of the MPPT Controller IC at node V(5,3) for Different Solar Irradiances at 30^0 C Solar Cell Temperature.
Corner Case: Slow-Fast (SF)

Irradiance (W/m^2)	Ideal Maximum Power (W)	Measured Actual Power (W)	Tracking Efficiency (%)
400	12.879	12.7683	99.14%
600	19.155	18.9831	99.13%
800	25.158	24.9770	99.28%
1000	30.859	30.5632	99.04%

Table 16
Photovoltaic Array Power of the MPPT Controller IC at node V(5,3) for Different Solar Irradiances at 20^0 C Solar Cell Temperature.
Corner Case: Slow-Slow (SS)

Irradiance (W/m^2)	Ideal Maximum Power (W)	Measured Actual Power (W)	Tracking Efficiency (%)
400	13.411	13.2695	98.94%
600	19.93	19.7661	99.18%
800	26.161	26.0594	99.61%
1000	32.076	29.9440	93.35%

Table 17
Photovoltaic Array Power of the MPPT Controller IC at node V(5,3) for Different Solar Irradiances at 25^0 C Solar Cell Temperature.
Corner Case: Slow-Slow (SS)

Irradiance (W/m^2)	Ideal Maximum Power (W)	Measured Actual Power (W)	Tracking Efficiency (%)
400	13.14	12.9957	98.90%
600	19.536	19.3114	98.85%
800	25.65	25.5531	99.62%
1000	31.456	29.5643	93.99%

Table 18
Photovoltaic Array Power of the MPPT Controller IC at node V(5,3) for Different Solar Irradiances at 30^0 C Solar Cell Temperature.
Corner Case: Slow-Slow (SS)

Irradiance (W/m^2)	Ideal Maximum Power (W)	Measured Actual Power (W)	Tracking Efficiency (%)
400	12.879	12.7360	98.89%
600	19.155	18.7818	98.05%
800	25.158	25.0941	99.75%
1000	30.859	28.7667	93.22%

VII. CONCLUSION

A 5V analogue RCC-based MPPT controller IC was presented to harvest maximum power from the solar panel at different process corners and temperature. The simulation results showed that at 400 W/m^2 low irradiance and 25 degrees Celsius temperature, the tracking efficiencies are 99.18%, 98.55%, 98.89%, 98.96%, and 98.90% at different process corners, typical-typical (TT), fast-fast (FF), fast-slow (FS), slow-fast (SF), and slow-slow (SS), respectively . This means that the proposed design of the MPPT controller can harvest almost 100% of the expected power from the solar panel.

ACKNOWLEDGEMENTS

The authors would like to extend their deepest and most profound appreciation to the colleagues and mentors from the Mapua Institute of Technology and Technological University of the Philippines who directly or indirectly helped them to make this study possible.

REFERENCES

[1] M. Glavin, W. G. Hurley. Battery management system for solar energy applications. *Universities Power Engineering Conference, 2006. UPEC'06. Proceedings of the 41st International*, 1 (2006) 79-83.

[2] Yuncong Jiang, Jaber A. Abu Qahouq, Ahmed Hassan, Emad Abdelkarem, and Mohamed Orabi. Load current based analog MPPT controller for PV solar systems. *Applied Power Electronics Conference and Exposition (APEC), 2012 Twenty-Seventh Annual* (2012) 911-914.

[3] T. Esram, P. L. Chapman. Comparison of photovoltaic array maximum power point tracking techniques. *IEEE Transactions on energy conversion*. 22(2)(2007) 439-449.

[4] Yan Hong Lim, D. C. Hamill. Simple maximum power point tracker for photovoltaic arrays. *Electronics letters* 36(11)(2000) 997-999.

[5] P. Midya, P. T. Krein, R. J. Turnbull, R. Reppa, J. Kimball. Dynamic maximum power point tracker for photovoltaic applications. *Power Electronics Specialists Conference, 1996. PESC'96* Record., 27th Annual IEEE, 2 (1996) 1710-1716.

[6] Yan Hong Lim, D. C. Hamill. Synthesis, simulation and experimental verification of a maximum power point tracker from nonlinear dynamics. *Power Electronics Specialists Conference, 2001. PESC. 2001 IEEE 32nd Annual*, 1(2001) 199-204.

[7] M. A. De Brito, L. P. Sampaio, G. Luigi, G. A. e Melo, C. A. Canesin. Comparative analysis of MPPT techniques for PV applications. *Clean Electrical Power (ICCEP), 2011 International Conference on*, (2011) 99-104.

[8] Zainal Salam, Jubaer Ahmed, Benny S. Merugu. The application of soft computing methods for MPPT of PV system: A technological and status review. *Applied Energy*. 107(2013) 135-148.

[9] Eltawil, M. A., Zhengming Zhao. MPPT techniques for photovoltaic applications. *Renewable and Sustainable Energy Reviews* 25 (2013) 793-813.

[10] Mohamed Orabi, Fatma Hilmy, Ahmed Shawky, Jaber A. Abu Qahouq, El-Sayed Hasaneen, Eman Gomaa. On-chip integrated power management MPPT controller utilizing cell-level architecture for PV solar system. *Solar Energy*. 117(2015) 10-28.

[11] Ahmed Shawky, Fatma Helmy, Mohamed Orabi, Jaber Abu Qahouq, and Zhigang Dang. On-chip integrated cell-level power management architecture with MPPT for PV solar system. Applied Power Electronics Conference and Exposition (APEC), *2014 Twenty-Ninth Annual IEEE*, (2014) 572-579.

[12] S. Ajay, A. Arunkumar, G. Deepika, S. Maneesha, and R. Ramaprabha. Compact Maximum Power Point Tracking of Solar Photovoltaic Systems Using Analog ICs. *India Educators' Conference (TIIEC),* 2013 Texas Instruments, (2013) 135-140.

[13] L. Castaner, S. Silvestre. Modelling photovoltaic systems using PSpice. John Wiley and Sons, (2002).